COLD SPRING HARBOR
Molecular Case Studies

RESEARCH REPORT

WISP3 mutation associated with pseudorheumatoid dysplasia

M. Reza Sailani,[1] James Chappell,[1] Inlora Jingga,[1] Anil Narasimha,[1] Amin Zia,[1] Janet Linnea Lynch,[1] Safoura Mazrouei,[2] Jonathan A. Bernstein,[3] Omid Aryani,[4,5] and Michael P. Snyder[1]

[1]Department of Genetics, Stanford University, Stanford, California 94304, USA; [2]Clinic of Internal Medicine, Department of Cardiology, University Heart Center, Jena University Hospital, 07747 Jena, Germany; [3]Department of Pediatrics, Stanford University, Stanford, California 94304, USA; [4]Department of Neuroscience, Iran University of Medical Sciences, Tehran 1449614535, Iran; [5]Endocrinology and Metabolic Research Institute, Tehran University of Medical Sciences, Tehran 1599666615, Iran

Abstract Progressive pseudorheumatoid dysplasia (PPD) is a skeletal dysplasia characterized by predominant involvement of articular cartilage with progressive joint stiffness. Here we report genetic characterization of a consanguineous family segregating an uncharacterized from of skeletal dysplasia. Whole-exome sequencing of four affected siblings and their parents identified a loss-of-function homozygous mutation in the *WISP3* gene, leading to diagnosis of PPD in the affected individuals. The identified variant (Chr6: 112382301; WISP3:c.156C>A p.Cys52*) is rare and predicted to cause premature termination of the *WISP3* protein.

[Supplemental material is available for this article.]

INTRODUCTION

Rare genetic conditions involving the skeletal system arise through misregulation in the process of skeletal development (cartilage and bone growth) and remain a diagnostic challenge because of the rarity of the disease and the heterogeneity in the phenotypes (Kornak and Mundlos 2003; Krakow and Rimoin 2010; Chen et al. 2016). Moreover, given the fact that some skeletal phenotypes are driven by several different genes, and that some genes can lead to a variety of different skeletal diseases, achieving a molecular diagnosis can be difficult. Correct diagnosis for progressive pseudorheumatoid dysplasia (PPD) is particularly challenging as it is very rare (~1 in a million) (Wynne-Davies et al. 1982; Garcia Segarra et al. 2012) and has similarities with other disorders (i.e., mucopolysaccharidosis, rheumatoid arthritis, and ankylosing spondylitis) (Spranger et al. 1983; Neerinckx et al. 2015).

RESULTS

Family Description

Here we report genetic characterization of a consanguineous family segregating PPD. Written informed consent was obtained for all participants. The institutional review boards of the Special Medical Center, Tehran, Iran and Stanford University reviewed the project. The family pedigree is shown in Figure 1A. Affected individuals underwent examination at the Special Medical Center for rare diseases, Tehran, Iran. The patients were asymptomatic at birth, with normal growth, development, and intelligence as well as no facial, joint, and

Corresponding authors:
mpsnyder@stanford.edu;
o_aryani@yahoo.com

Ontology terms: multiple skeletal anomalies; spondyloepimetaphyseal dysplasia

Published by Cold Spring Harbor Laboratory Press

doi: 10.1101/mcs.a001990

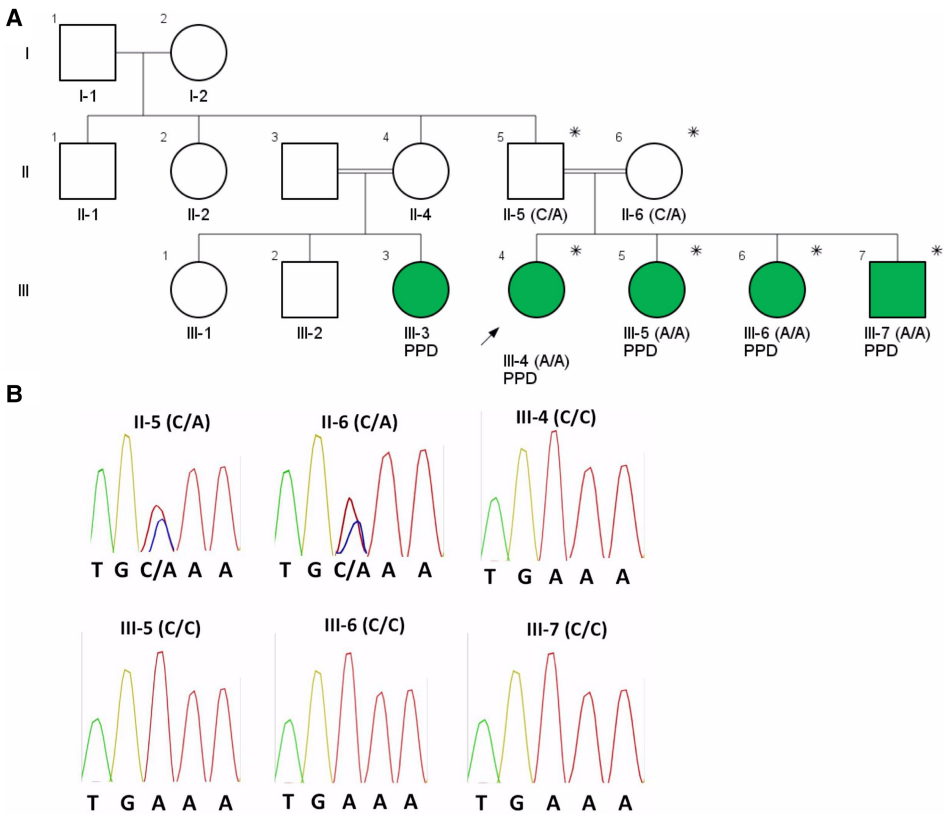

Figure 1. (*A*) Pedigree structure of the PPD family. The star shows family members from whom DNA samples were available and sequenced. (*B*) Sanger sequencing traces (TGC/AAA) showing the c.156C>A; p.Cys52* mutation in the *WISP3* gene. The segregation of this mutation has been confirmed in six available DNA samples from this family.

skeletal system deformity. However, the disease started to manifest at 4–6 years of age in affected individuals and progressively worsened (Table 1). Presenting findings included the enlargement of joints—first in the large joints of the limbs (knees, ankles, and elbow) and then a knobby appearance of the proximal interphalangeal joints of the hands. By the age of 10 yr, a knobby appearance in the metacarpophalangeal and distal interphalangeal joints of the hands was present, as well as the involvement of the spine (mild abnormality). In early adolescence, some affected individuals displayed gait disturbances because of knee deformity and some contracture. In late adolescence and beyond, flexion contracture and stiffness in the large joints had developed (knees, elbows, and hip) and the fingers and toes became short (camptodactylic) (Table 1). Moreover, a skeletal survey showed degenerative changes with generalized osteopenia with the presence of unfused epiphyses in the vertebrae. All together, these clinical data indicate a skeletal dysplasia; however, because of heterogeneity in skeletal abnormalities, it was challenging to precisely make a diagnosis for this abnormality. Therefore, we applied a WES approach to identify the casual gene and came up with a precise diagnosis.

Exome-Sequencing Results

WES to a mean coverage of >80× (Individuals 1.2, 2.1, 2.2, 2.3, and 2.4 of Fig. 1) was performed (Supplemental Table S1). We identified 163,116 variants that are shared in all the

Table 1. Family phenotypic features

Individual	II-5 (father)	II-6 (mother)	III-4	III-5	III-6	III-7
Sex	Male	Female	Female	Female	Female	Male
Intelligence	Normal	Normal	Normal	Normal	Normal	Normal
Birth weight	Normal	Normal	Normal	Normal	Normal	Normal
Neonatal history	Normal	Normal	Normal	Normal	Normal	Normal
Disease diagnosis	Normal	Normal	PPD	PPD	PPD	PPD
Age of onset	NA	NA	6	6	4	4
Enlargement of joints (4–6-yr-old)	NA	NA	Yes	Yes	Yes	Yes
Enlarged epiphyses (4–6-yr-old)	NA	NA	Yes	Yes	Yes	Yes
Enlargement of the proximal femoral epiphysis (4–6-yr-old)	NA	NA	Yes	Yes	Yes	Yes
Knobby appearance of distal interphalangeal joints (4–6-yr-old)	NA	NA	Yes	Yes	Yes	Yes
Generalized osteopenia (4–6-yr-old)	NA	NA	Yes	Yes	Yes	Yes
Enlarged metacarpophalangeal joints (9–10-yr-old)	NA	NA	Yes	Yes	Yes	Yes
Knobby appearance in the metacarpophalangeal (9–10-yr-old)	NA	NA	Yes	Yes	Yes	Yes
Decreased cervical spine mobility (9–10-yr-old)	NA	NA	Yes	Yes	Yes	Yes
Gait disturbance (10–14-yr-old)	NA	NA	No	No	Yes	Yes
Flexion contracture (15–19-yr-old)	NA	NA	Yes	Yes	Yes	Yes
Stiffness in the large joints (15–19-yr-old)	NA	NA	Yes	Yes	Yes	Yes
Camptodactyly (15–19-yr-old)	NA	NA	Yes	Yes	Yes	Yes
Kyphoscoliosis (15–19-yr-old)	NA	NA	Yes	Yes	Yes	Yes
Joint stiffness (15–19-yr-old)	NA	NA	Yes	Yes	Yes	Yes
Joint swelling (15–19-yr-old)	NA	NA	Yes	Yes	Yes	Yes
Chest deformity (15–19-yr-old)	NA	NA	Yes	Yes	Yes	Yes
Walking difficulties (15–19-yr-old)	NA	NA	Yes	Yes	Yes	Yes
Easily fatigued	NA	NA	ND	ND	ND	ND

NA, not applied; ND, not determined; PPD, progressive pseudorheumatoid dysplasia.

family members and have a genotype quality score of >20 (Table 2). Based on the pedigree, we predicted the disease would follow an autosomal recessive pattern. Thus, we analyzed variants that were homozygous in affected individuals but heterozygous in the healthy parents. Of note, 1064 variants (151 missense variants, 359 variants in 3′ UTRs and 5′ UTRs, 43 frameshift variants, 34 in-frame deletions and insertions, 43 splicing event–related variants, 276 intergenic variants, 321 intronic variants, 101 synonymous variants, and 12 stop gain, stop lost, and stop retained variants) were identified. We then selected variants with a minor allele frequency (MAF) of <0.01 in public databases: dbSNP Common 144 (Database of Single Nucleotide Polymorphism, NCBI), 1000 Genome project phase 3 (www.1000genomes.org), Exome Aggregation Consortium version 0.3 (ExAC; http://exac.broadinstitute.org/), NHLBI GO Exome Sequencing Project (ESP; http://evs.gs.washington.edu/EVS/). These filtering steps resulted in identifying 286 homozygous variants, of which 26 are exonic and only one variant was predicted to be pathogenic (stop-gain variant)

Table 2. Variant filtering steps

Individual ID	I-2	II-1	II-2	II-3	II-4
Shared variants			163,116		
Homozygote variants in affected but heterozygote variants in parents			1064		
1KG MAF < 0.01			373		
ExAC MAF < 0.01			325		
dbSNP 144 MAF < 0.01			322		
NHLBI MAF < 0.01			320		
UK 10K twins			286		
UK 10K ALSPAC			286		
Exonic variants			26		
Pathogenic (missense or stop gain/loss)			1		
Candidate			Chr6:112,382,301; WISP3; c.156C>A; p.Cys52*		

MAF, minor allele frequency; 1KG, 1000 Genomes project phase 3; ExAC, Exome Aggregation Consortium version 0.3; dbSNP 144, Database of Single Nucleotide Polymorphism, NCBI; NHLBI, Exome Variant Server, NHLBI GO Exome Sequencing Project (ESP).

(Table 2). The identified variant occurs in the exon three of *WISP3* gene (WISP3;c.156C>A; p.Cys52*), is rare (MAF of 0.0008% in ExAC; 0.04% in dbSNP 144; no homozygotes), and is predicted to be deleterious (Table 3). We confirmed the homozygosity of this variant by Sanger sequencing (Fig. 1B) using 5′GGCCTGGAGAAGTGTCAGAT3′ and 5′GTCTCGTA CCTAGGCCTGTC3′ for PCR amplification and 5′GTCTCGTACCTAGGCCTGTC3′ as a Sanger sequencing primer. We showed that the variant segregates in the family, as all four affected individuals have the homozygous mutation, whereas their parents are heterozygous (Fig. 1B).

DISCUSSION

In this study, we employed whole-exome sequencing to identify the underlying genetic variants associated with a rare uncharacterized form of skeletal dysplasia. Abnormalities involving the skeletal system remain a diagnostic challenge because of the heterogeneity of skeletal system diseases. Moreover, given the fact that some skeletal phenotypes are driven by several different genes, and that some genes can lead to a variety of different skeletal diseases, achieving a molecular diagnosis can be quite difficult. To overcome this challenge, we combined the clinical data from a family segregating a rare uncharacterized form of skeletal dysplasia with a comprehensive WES approach. We have sequenced all four affected siblings and their parents to identify the causal mutation associated with this skeletal dysplasia in order to make a better diagnostic. Our study reports a homozygote mutation for rs121908901; WISP3; c.156C>A; p.Cys52*, which introduces a stop codon in the IGFBP

Table 3. Summary of the variant reported in this study

Gene	Chr	HGVS DNA reference	HGVS protein reference	Predicted effect	Variant type	dbSNP ID	Genotype	ClinVar accession	ExAC MAF	Inheritance
WISP3	Chr6: 112382301	NM_003880.3: c.156C>A	NP_003871.1: p.Cys52Ter	Cys52*	Stop-gained	rs121908901	Homozygous	SVC000607728	6.056e-05	Homozygous recessive

domain of the WISP3 protein. Previously, Hurvitz et al. 1999 reported a compound heterozygote involving the same variant in a French family with progressive pseudorheumatoid arthropathy of childhood (Hurvitz et al. 1999).

WISP3

The *WNT1 Inducible Signaling Pathway Protein 3* (*WISP3*) gene encodes a member of the connective tissue growth factor (CTGF) family of secreted cysteine-rich, glycosylated proteins that play a multitude of roles in cell growth and differentiation (Bork 1993). The first clinical link between *WISP3* and PPD was demonstrated by linkage studies in consanguineous families segregating PPD, which mapped the candidate region to a 3-cM interval between D6S1594 and D6S432 microsatellite markers on Chromosome 6q22 (el-Shanti et al. 1998; Fischer et al. 1998). One year later, Hurvitz et al. (1999) identified mutations in the linkage region, specifically in *WISP3*, as the strongest candidates to cause this autosomal recessive condition.

The Spectrum of Mutations in *WISP3*

The WISP3 protein contains a signaling peptide (SP) and four conserved cysteine-rich domains that are differentially affected by mutations (Fig. 2). Figure 2 shows a schematic representation of the WISP3 protein domains, and Table 4 represents a comprehensive representation of the mutation spectrum of WISP3 in the literature (Table 4). The insulin-like growth factor–binding domain (IGFBP) has been shown to bind IGF-1 to inhibit signaling, and mutations within have been shown to sensitize articular chondrocytes to IGF-1, causing hypertrophy and diminished production of collagen types II and IX (Liao et al. 2004; Repudi et al. 2013). As shown in Figure 2, this domain contains the highest number of described deleterious mutations (34%), as well as the most affected families. In contrast, the von Willebrand factor type C module (VWC) domain contains only ~7% of described mutations and has the least evidence regarding its possible function in PPD. Although not demonstrated in *WISP3*, the VWC domain has been shown to interact with BMP and TGF-β family members and to promote oligomerization in other related family members (Holbourn et al. 2008). The thrombospondin domain (TSP) has been identified as a negative regulator of Slug/Notch1 signaling and thus as an anti-angiogenic factor in breast cancer epithelial cells (Huang et al. 2016). Suppression of Notch is likely important in chondrocytes as well, given the observation that Notch signaling promotes ossification and osteoarthritis (Hosaka et al. 2013). This domain contains the second highest number, ~31% of the described deleterious mutations in PPD. Finally, the carboxy-terminal cystine knot–like domain (CTCK) is a commonly identified motif found in proteins that form dimers and bind a variety of ligands (Isaacs 1995; Holbourn et al. 2008). For example, in a *WISP3*-related factor called CCN2

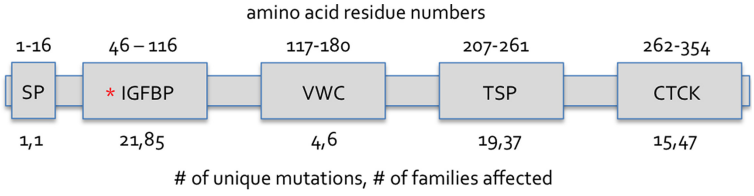

Figure 2. Schematic of the WISP3 protein. Amino acid residue numbers are indicated above each domain. The number of unique mutations and the number of affected families described are indicated below the domains. WISP3 contains a signaling peptide (SP) and four conserved cysteine-rich domains: insulin-like growth factor–binding domain (IGFBP), von Willebrand factor type C module (VWC), thrombospondin domain (TSP), and carboxy-terminal cystine knot–like domain (CTCK). The * indicates where c.156C>A occurs.

Table 4. Spectrum of *WISP3* pathogenic mutations

Variant	HGMD accession	dbSNP ID	Protein change	Citation	Population	No. of families
c.43_44delGC	CD991937	–	p.Ala15Thrfs*17	Hurvitz et al. 1999	USA	1
c.48+2dupT	CI994276	rs797044439	splicing: 2IVS+2	Hurvitz et al. 1999; Garcia Segarra et al. 2012	Jordan, Morocco	2
c.49-763G>T	CS126440	-	splicing: IVS2 -763	Garcia Segarra et al. 2012	Belgium	1
c.49-1G>A	CS159581	rs781864926	splicing: IVS2 -1	Bhavani et al. 2015	India	1
c.105dupT	CI151711	–	p.Gly36fs*10	Liu et al. 2015	China	1
c.136C>T	CM091536	–	p.Gln46*	Yue et al. 2009; Ye et al. 2012; Yu et al. 2015	China	3
c.156C>A	CM991252	rs121908901	p.Cys52*	Hurvitz et al. 1999; Delague et al. 2005; Garcia Segarra et al. 2012; Rai et al. 2016; Temiz et al. 2011; Bhavani et al. 2015; Madhuri et al. 2016	Italy, France, Lebanon, Syria, Turkey, Germany, India	33
c.182G>T	CM126432	–	p.Cys61Phe	Garcia Segarra et al. 2012	Poland	1
c.185delC	CD126426	–	p.Pro62Leufs*4	Garcia Segarra et al. 2012	Turkey	2
c.190G>A	CM166919	–	p.Gly64Arg	Montane et al. 2016	Ecuador	1
c.197G>A	CM126433	rs782172825	p.Ser66Asn	Garcia Segarra et al. 2012; Montane et al. 2016	USA, Italy, Ecuador	3
c.232T>C	CM991253	rs121908902	p.Cys78Arg	Hurvitz et al. 1999	France	1
c.233G>A	CM129533	–	p.Cys78Tyr	Dalal 2012; Ekbote et al. 2013; Bhavani et al. 2015; Madhuri et al. 2016	India	9
c.236_237CC>AA	CX126439	–	p.Ala79Glu	Garcia Segarra et al. 2012	Italy	1
c.246delA	CD991938	rs797044438	p.Glu84Lysfs*21	Hurvitz et al. 1999	Saudi Arabia, Jordan	3
c.248G>A	CM129541	rs147337485	p.Gly83Glu	Delague et al. 2005; Dalal et al. 2012; Ekbote et al. 2013; Rai et al. 2016; Temiz et al. 2011	Lebanon, Syria, India	10
c.296A>T	CM159583	–	p.Tyr99Phe	Bhavani et al. 2015	India	1
c.298T>A	CM159594	–	p.Cys100Ser	Bhavani et al. 2015	India	1
c.327C>A	CM126423	–	p.Tyr109*	Garcia Segarra et al. 2012	Turkey	3
c.340T>C	CM129534	–	p.Cys114Arg	Dalal et al. 2012	India	1
c.341G>A	–	–	p.Cys114Tyr	Yue et al. 2009	China	2
c.342_343delTG	CD126427	–	p.Ala115Ilefs*16	Garcia Segarra et al. 2012	Turkey	1
c.341G>A	CM091537	–	p.Cys114Tyr	Yue et al. 2009	China	1
c.342T>G	CM118811	–	p.Cys114Trp	Sun et al. 2012; Ye et al. 2012; Liu et al. 2015; Yan et al. 2016; Yu et al. 2015	China	5
c.346+1G>T	–	–	p.Tyr109_Met195delins9	Garcia Segarra et al. 2012	Turkey	1
c.347-2A>G	CS159640	–	splicing: IVS3 -2	Bhavani et al. 2015	India	1
c.347-3_347-1delCAG	CD159582	–	-	Bhavani et al. 2015	India	1
c.346+1G>T	CS126438	–	splicing: IVS3 +1	Garcia Segarra et al. 2012	Turkey	1
c.348C>A	CM129535	–	p.Tyr116*	Dalal et al. 2012; Madhuri et al. 2016	India	2
c.433T>C	CM129536	–	p.Cys145Arg	Dalal et al. 2012	India	2

(*Continued on next page.*)

Table 4. (*Continued*)

Variant	HGMD accession	dbSNP ID	Protein change	Citation	Population	No. of families
c.434G>A	CM991254	rs121908899	p.Cys145Tyr	Hurvitz et al. 1999; Garcia Segarra et al. 2012	Italy	2
c.530C>A	CM159598	–	p.Ser177*	Bhavani et al. 2015	India	1
c.536_537delGT	CD053623	–	p.Cys179*	Delague et al. 2005	Syria	1
c.589G>C	CS053500	–	Splicing: IVS4 ds -1	Delague et al. 2005	Syria	1
c.589+1G>A	CS1610143	rs879255273	Splicing: IVS4 ds +1	Rai et al. 2016	India	1
c.589+27C>G	CS126441	–	Splicing: IVS4 ds +27	Garcia Segarra et al. 2012	Italy	1
c.594_598delTAGAA	CD1610848	–	p.Tyr198*	Madhuri et al. 2016	India	1
c.621_622delAAinsT	CX126431	–	p.Lys207Asnfs025	Garcia Segarra et al. 2012	USA	1
c.624_625insA	–	–	p.Cys209Metfs*21	Ye et al. 2010, 2012	China	3
c.624delA	CD151709	–	p.Lys208fs*24	Liu et al. 2015	China	1
c.624dupA	CI105183	–	p.Cys209Metfs	Ye et al. 2010, 2012	China	1
c.625dupT	CI1615597	–	p.Cys209Leufs*21	Yan et al. 2016	China	1
c.667T>G	CM118812	-	p.Cys223Gly	Ye et al. 2012; Luo et al. 2015; Yan et al. 2016; Yu et al. 2015	China	4
c.670G>A	CM126437	–	p.Gly224Arg	Garcia Segarra et al. 2012	Italy	1
c.677G>T	CM126434	–	p.Gly226Val	Garcia Segarra et al. 2012; Madhuri et al. 2016	UK, India	2
c.682T>C	CM129537	–	p.Ser228Pro	Dalal et al. 2012; Ekbote et al. 2013	India	2
c.682_686dupTCTAA	CI159616	–	p.Arg230Leufs*4	Bhavani et al. 2015	India	1
c.684dupT	CI159608	–	p.Asn229*	Bhavani et al. 2015	India	1
c.708dupC	CI126430	–	p.Asn237Glnfs*3	Garcia Segarra et al. 2012	Turkey	2
c.716_722del	CD124723	–	p.Glu239fs*16	Sun et al. 2012	China	1
c.719_725delTGAGAAA	CD124723	–	-	Sun et al. 2012		
c.725_726delAA	CD126429	–	p.Lys242Argfs*36	Garcia Segarra et al. 2012	Italy	2
c.727_731delGAGAA	CD126428	–	p.Glu243Lysfs*34	Garcia Segarra et al. 2012	Turkey	3
c.729_735delGAAAAGA	CD105182	–	p.Glu243Aspfs*13	Ye et al. 2010, 2012	China	5
c.740_741delGT	CD044991	–	p.Cys247Leufs*31	Ehl et al. 2004; Dalal et al. 2012; Garcia Segarra et al. 2012; Bhavani et al. 2015	Caucasian, India, Germany	4
c.756C>A	CM153375	–	p.Cys252*	Luo et al. 2015	China	1
c.783+1_783 +6delGTAAAG	CD159627	–	p.Ile260Asnfs*17	Bhavani et al. 2015	India	1
c.802T>G	CM129538	–	p.Cys268Gly	Dalal et al. 2012	India	1
c.805delC	CD159638	–	p.Q269Nfs*44	Bhavani et al. 2015	India	1
c.840delT	HD040019	rs797044440	p.Phe280Leufs*33	Liao et al. 2004; Peng et al. 2004; Yang et al. 2013	China	3
c.850G>T	CM126424	–	p.Gly284*	Garcia Segarra et al. 2012	Turkey	1
c.857C>G	CM126425	–	p.Ser286*	Garcia Segarra et al. 2012; Yu et al. 2015	Turkey, China	2
c.862_863dupAC	CI992094	rs863223286	p.Gln289Leufs*25	Hurvitz et al. 1999	USA	1
c.866_867insA	-	–	p.Gln289fs*31	Sun et al. 2012; Ye et al. 2012	China	2
c.866dupA	CI105184	–	p.Ser290Glufs*13	Ye et al. 2010, 2012; Sun et al. 2012; Yu et al. 2015	China, Italy	9

(*Continued on next page.*)

Table 4. (*Continued*)

Variant	HGMD accession	dbSNP ID	Protein change	Citation	Population	No. of families
c.868_869delAG	CD991939	–	p.Ser290Leufs*12	Hurvitz et al. 1999; Garcia Segarra et al. 2012	Iran, Italy	2
c.947_951delAATTT	CD129539	–	p.Gln316Argfs*5	Dalal et al. 2012	India	1
c.993G>A	CM991255	rs121908900	p.Trp331*	Hurvitz et al. 1999	Italy	1
c.1000T>C	HM040052	rs121908903	p.Ser334Pro	Liao et al. 2004; Sun et al. 2012; Peng et al. 2004	China	3
c.1004G>A	CM126435	–	p.Cys335Tyr	Garcia Segarra et al. 2012	Italy	1
c.1010G>A	CM126436	–	p.Cys337Tyr	Dalal et al. 2012; Garcia Segarra et al. 2012; Ekbote 2013; Bhavani et al. 2015; Madhuri et al. 2016	India	18
c.1013A>T	CM078552	rs587640965	p.Gln338Leu	Nakamura et al. 2007	Japan	1

the cystine knot domain interacts with BMP-2 to activate a signaling program that promotes mature chondrocytes (Maeda et al. 2009). This domain has the third highest number of deleterious mutations at 25%.

In conclusion, our study, in line with previous studies (Hurvitz et al. 1999; Nakamura et al. 2007; Neerinckx et al. 2015; Yu et al. 2015; Rai et al. 2016; Yan et al. 2016), provides further evidence of the essential role of *WISP3* in postnatal skeletal growth and cartilage homeostasis in humans.

METHODS

Exome Sequencing and Variant Calling

Exome capture, library preparation, and sequencing, as well as data analysis, were performed as previously described (Reza Sailani et al. 2017). Briefly, exome capture and library preparation were performed using the Agilent SureSelectXT HumanAllExon V5 (product no. 5190–4631). Two micrograms of gDNA was sheared to a peak size of 150–200 bp using the Covaris instrument. Fragmented genomic DNA was purified using Agencourt AmpPure XP beads (Beckman Coulter) to remove fragments of <100 bp. Then, according to the manufacturer's instructions, the purified DNA fragments were then end-repaired, A-tailed, and ligated to indexing-specific paired-end adaptors using the Agilent SureSelect Library Prep Kit, ILM.

The adaptor-ligated libraries were amplified for five cycles with the SureSelect Primer and the SureSelect Indexing Pre-Capture reverse primer. The PCRs were cleaned using the Agencourt AMPure XP beads. To capture exonic regions, 500 ng of each prepared library was hybridized to biotinylated cRNA oligonucleotides for 24 h at 65°C. The captured libraries were pulled down using Dynabeads MyOne Streptavidin T1 (Invitrogen). A post-capture PCR was then performed to amplify the captured libraries and to add the barcode sequences for multiplex sequencing for 14 cycles. Afterward, amplified libraries were purified with AMPure XP Beads. Qubit fluorometer and Bioanalyzer high-sensitivity chips were used to determine the final concentration of each captured library. One library was prepared per sample. Libraries were pooled in three and were paired-end sequenced on a single Illumina HiSeq lane at the Stanford Center for Genomics and Personalized Medicine according to standard protocols.

Bioinformatics Analyses

Raw FASTQ files were aligned to the human genome (hg19 version), and SNPs and indels were called using the BINA pipeline (http://www.bina.com). For variant filtering, Golden Helix VarSeq software (http://goldenhelix.com/products/VarSeq/) was used.

Sanger Sequencing

We used 5′GGCCTGGAGAAGTGTCAGAT3′ and 5GTCTCGTACCTAGGCCTGTC3′ for PCR amplification of the variant sequence. PCR amplification was performed using following reagents: 25 µl REDTaq ReadyMix PCR Reaction Mix (Sigma-Aldrich), 1 µl forward primer (10 µM), 1 µl reverse primer (10 µM), 1 µl DNA (50 ng/µl), and 22 µl of water per PCR reaction. An initial denaturation step for 3 min at 94° was followed by 35 cycles of 30 sec at 94°, 30 sec at 57°, 30 sec at 72°, and the process completed by a final extension for 7 min at 72°. The PCR amplification resulted in a single DNA band on a standard 1% agarose gel and was purified by Agencourt AMPure XP beads (Beckman Coulter, Inc) before submitting for Sanger sequencing. The reverse primer 5′GTCTCGTACCTAGGCCTGTC3′ was used as sequencing primer. Sanger sequencing was carried out by the Stanford PAN facility using ABI 3130xl Genetic Analyzer.

ADDITIONAL INFORMATION

Data Deposition and Access

The family consented to the genetic study and publication of the genetic and clinical results. The exome-sequencing data have been deposited in the National Center for Biotechnology Information (NCBI) Sequence Read Archive (SRA) (http://www.ncbi.nlm.nih.gov/sra/) under SRA Study SRP106899. The variant was submitted to ClinVar (http://www.ncbi.nlm.nih.gov/clinvar/) and can be found under accession number SCV000607728.

Ethics Statement

All participants, or their legal guardian, provided written and informed consent. The institutional review boards of the Special Medical Center, Tehran, Iran and Stanford University reviewed the project. All the affected individuals underwent examination at the Special Medical Center, Tehran, Iran.

Competing Interest Statement

Michael P. Snyder is a cofounder of Personalis and a member of the scientific advisory boards of Personalis and Genapsys.

Referees

Peter N. Robinson
Anonymous

Received March 12, 2017; accepted in revised form September 28, 2017.

Acknowledgments

We thank the Stanford Center for Genomics and Personalized Medicine for their sequencing services.

Funding

M.R.S. is supported by a grant from the Swiss National Science Foundation (SNSF). Work in the Snyder laboratory is supported by National Institutes of Health (NIH) grants to M.P.S. (1P50HG00773501 and 8U54DK10255602).

REFERENCES

Bhavani GS, Shah H, Dalal AB, Shukla A, Danda S, Aggarwal S, Phadke SR, Gupta N, Kabra M, Gowrishankar K, et al. 2015. Novel and recurrent mutations in *WISP3* and an atypical phenotype. *Am J Med Genet A* **167A:** 2481–2484.

Bork P. 1993. The modular architecture of a new family of growth regulators related to connective tissue growth factor. *FEBS Lett* **327:** 125–130.

Chen C, Jiang Y, Xu C, Liu X, Hu L, Xiang Y, Chen Q, Chen D, Li H, Xu X, et al. 2016. Skeleton Genetics: a comprehensive database for genes and mutations related to genetic skeletal disorders. *Database (Oxford)* **2016:** baw127.

Dalal A, Bhavani GS, Togarrati PP, Bierhals T, Nandineni MR, Danda S, Danda D, Shah H, Vijayan S, Gowrishankar K, et al. 2012. Analysis of the *WISP3* gene in Indian families with progressive pseudorheumatoid dysplasia. *Am J Med Genet A* **158A:** 2820–2828.

Delague V, Chouery E, Corbani S, Ghanem I, Aamar S, Fischer J, Levy-Lahad E, Urtizberea JA, Megarbane A. 2005. Molecular study of *WISP3* in nine families originating from the Middle-East and presenting with progressive pseudorheumatoid dysplasia: identification of two novel mutations, and description of a founder effect. *Am J Med Genet A* **138A:** 118–126.

Ehl S, Uhl M, Berner R, Bonafé L, Superti-Furga A, Kirchhoff A. 2004. Clinical, radiographic, and genetic diagnosis of progressive pseudorheumatoid dysplasia in a patient with severe polyarthropathy. *RheumatolInt* **24:** 53–56.

Ekbote AV, Danda D, Kumar S, Danda S, Madhuri V, Gibikote S. 2013. A descriptive analysis of 14 cases of progressive-psuedorheumatoid-arthropathy of childhood from south India: review of literature in comparison with juvenile idiopathic arthritis. *Semin Arthritis Rheum* **42:** 582–589.

el-Shanti H, Murray JC, Semina EV, Beutow KH, Scherpbier T, al-Alami J. 1998. Assignment of gene responsible for progressive pseudorheumatoid dysplasia to Chromosome 6 and examination of *COL10A1* as candidate gene. *Eur J Hum Genet* **6:** 251–256.

Fischer J, Urtizberea JA, Pavek S, Vandiedonck C, Bruls T, Saker S, Alkatip Y, Prud'homme JF, Weissenbach J. 1998. Genetic linkage of progressive pseudorheumatoid dysplasia to a 3-cM interval of Chromosome 6q22. *Hum Genet* **103:** 60–64.

Garcia Segarra N, Mittaz L, Campos-Xavier AB, Bartels CF, Tuysuz B, Alanay Y, Cimaz R, Cormier-Daire V, Di Rocco M, Duba HC, et al. 2012. The diagnostic challenge of progressive pseudorheumatoid dysplasia (PPRD): a review of clinical features, radiographic features, and *WISP3* mutations in 63 affected individuals. *Am J Med Genet C Semin Med Genet* **160C:** 217–229.

Holbourn KP, Acharya KR, Perbal B. 2008. The CCN family of proteins: structure-function relationships. *Trends Biochem Sci* **33:** 461–473.

Hosaka Y, Saito T, Sugita S, Hikata T, Kobayashi H, Fukai A, Taniguchi Y, Hirata M, Akiyama H, Chung UI, et al. 2013. Notch signaling in chondrocytes modulates endochondral ossification and osteoarthritis development. *Proc Natl Acad Sci* **110:** 1875–1880.

Huang W, Martin EE, Burman B, Gonzalez ME, Kleer CG. 2016. The matricellular protein CCN6 (WISP3) decreases Notch1 and suppresses breast cancer initiating cells. *Oncotarget* **7:** 25180–25193.

Hurvitz JR, Suwairi WM, Van Hul W, El-Shanti H, Superti-Furga A, Roudier J, Holderbaum D, Pauli RM, Herd JK, Van Hul EV, et al. 1999. Mutations in the CCN gene family member *WISP3* cause progressive pseudorheumatoid dysplasia. *Nat Genet* **23:** 94–98.

Isaacs NW. 1995. Cystine knots. *Curr Opin Struct Biol* **5:** 391–395.

Kornak U, Mundlos S. 2003. Genetic disorders of the skeleton: a developmental approach. *Am J Hum Genet* **73:** 447–474.

Krakow D, Rimoin DL. 2010. The skeletal dysplasias. *Genet Med* **12:** 327–341.

Liao EY, Peng YQ, Zhou HD, Mackie EJ, Li J, Hu PA, Zhou SH, Wen GB, Zhai MX, Luo XH, et al. 2004. Gene symbol: *WISP3*. Disease: spondyloepiphyseal dysplasia tarda with progressive arthropathy. *Hum Genet* **115:** 169.

Liu L, Li N, Zhao Z, Li W, Xia W. 2015. Novel *WISP3* mutations causing spondyloepiphyseal dysplasia tarda with progressive arthropathy in two unrelated Chinese families. *Joint Bone Spine* **82:** 125–128.

Luo H, Shi C, Mao C, Jiang C, Bao D, Guo J, Du P, Wang Y, Liu Y, Liu X, et al. 2015. A novel compound *WISP3* mutation in a Chinese family with progressive pseudorheumatoid dysplasia. *Gene* **564:** 35–38.

Madhuri V, Santhanam M, Rajagopal K, Sugumar LK, Balaji V. 2016. *WISP3* mutational analysis in Indian patients diagnosed with progressive pseudorheumatoid dysplasia and report of a novel mutation at pY198. *Bone Joint Res* **5:** 301–306.

Maeda A, Nishida T, Aoyama E, Kubota S, Lyons KM, Kuboki T, Takigawa M. 2009. CCN family 2/connective tissue growth factor modulates BMP signalling as a signal conductor, which action regulates the proliferation and differentiation of chondrocytes. *J Biochem* **145:** 207–216.

Montane LS, Marin OR, Rivera-Pedroza CI, Vallespin E, Del Pozo A, Heath KE. 2016. Early severe scoliosis in a patient with atypical progressive pseudorheumatoid dysplasia (PPD): identification of two *WISP3* mutations, one previously unreported. *Am J Med Genet A* **170:** 1595–1599.

Nakamura Y, Weidinger G, Liang JO, Aquilina-Beck A, Tamai K, Moon RT, Warman ML. 2007. The CCN family member Wisp3, mutant in progressive pseudorheumatoid dysplasia, modulates BMP and Wnt signaling. *J Clin Invest* **117:** 3075–3086.

Neerinckx B, Thues C, Wouters C, Lechner S, Westhovens R, Van Esch H. 2015. A homozygous deletion of exon 1 in *WISP3* causes progressive pseudorheumatoid dysplasia in two siblings. *Hum Genome Var* **2:** 15049.

Peng YQ, Liao EY, Gu HM, Wei QY, Zhou HD, Li J, Xie H, Zhai MX, Tan LH, Luo XH, et al. 2004. [Pathology and molecular pathogenesis of spondyloepiphyseal dysplasia tarda with progressive arthropathy caused by compound CCN6 heterogeneous gene mutations]. *Zhonghua Yi Xue Za Zhi* **84:** 1796–1803.

Rai E, Mahajan A, Kumar P, Angural A, Dhar MK, Razdan S, Thangaraj K, Wise CA, Ikegawa S, Pandita KK, et al. 2016. Whole exome screening identifies novel and recurrent *WISP3* mutations causing progressive pseudorheumatoid dysplasia in Jammu and Kashmir-India. *Sci Rep* **6:** 27684.

Repudi SR, Patra M, Sen M. 2013. WISP3–IGF1 interaction regulates chondrocyte hypertrophy. *J Cell Sci* **126:** 1650–1658.

Reza Sailani M, Jahanbani F, Nasiri J, Behnam M, Salehi M, Sedghi M, Hoseinzadeh M, Takahashi S, Zia A, Gruber J, et al. 2017. Association of AHSG with alopecia and mental retardation (APMR) syndrome. *Hum Genet* **136:** 287–296.

Spranger J, Albert C, Schilling F, Bartsocas C, Stoss H. 1983. Progressive pseudorheumatoid arthritis of childhood (PPAC). A hereditary disorder simulating rheumatoid arthritis. *Eur J Pediatr* **140:** 34–40.

Sun J, Xia W, He S, Zhao Z, Nie M, Li M, Jiang Y, Xing X, Wang O, Meng X, et al. 2012. Novel and recurrent mutations of *WISP3* in two Chinese families with progressive pseudorheumatoid dysplasia. *PLoS One* **7:** e38643.

Temiz F, Ozbek MN, Kotan D, Sangun O, Mungan NO, Yuksel B, Topaloglu AK. 2011. A homozygous recurring mutation in *WISP3* causing progressive pseudorheumatoid arthropathy. *J Pediatr Endocrinol Metab* **24:** 105–108.

Wynne-Davies R, Hall C, Ansell BM. 1982. Spondylo-epiphysial dysplasia tarda with progressive arthropathy. A "new" disorder of autosomal recessive inheritance. *J Bone Joint Surg Br* **64:** 442–445.

Yan W, Dai J, Xu Z, Shi D, Chen D, Xu X, Song K, Yao Y, Li L, Ikegawa S, et al. 2016. Novel *WISP3* mutations causing progressive pseudorheumatoid dysplasia in two Chinese families. *Hum Genome Var* **3:** 16041.

Yang X, Song Y, Kong Q. 2013. Diagnosis and surgical treatment of progressive pseudorheumatoid dysplasia in an adult with severe spinal disorders and polyarthropathy. *Joint Bone Spine* **80:** 650–652.

Ye J, Zhang HW, Wang T, Cao LF, Qiu WJ, Han LS, Zhang YF, Gu XF.2010. Clinical diagnosis and *WISP3* gene mutation analysis for progressive pseudorheumatoid dysplasia. *Zhonghua Er Ke Za Zhi* **48:** 194–198.

Ye J, Zhang HW, Qiu WJ, Han LS, Zhang YF, Gong ZW, Gu XF. 2012. Patients with progressive pseudorheumatoid dysplasia: from clinical diagnosis to molecular studies. *Mol Med Rep* **5:** 190–195.

Yu Y, Hu M, Xing X, Li F, Song Y, Luo Y, Ma H. 2015. Identification of a mutation in the *WISP3* gene in three unrelated families with progressive pseudorheumatoid dysplasia. *Mol Med Rep* **12:** 419–425.

Yue H, Zhang ZL, He JW. 2009. Identification of novel mutations in *WISP3* gene in two unrelated Chinese families with progressive pseudorheumatoid dysplasia. *Bone* **44:** 547–554.